RESEARCH ARTICLE

Altered Corticomotor-Cerebellar Integrity in Young Ataxia Telangiectasia Patients

Ishani Sahama, BSc. Hons,[1] Kate Sinclair, MD,[2] Simona Fiori, MD,[3] Kerstin Pannek, PhD,[4] Martin Lavin, PhD,[5,6] and Stephen Rose, PhD[4]*

[1]*The University of Queensland, School of Medicine, Brisbane, Australia*
[2]*Neurology, The Royal Children's Hospital, Brisbane, Australia*
[3]*IRCCS Stella Maris, Calambrone, Pisa, Italy*
[4]*Commonwealth Scientific and Industrial Research Organization, Centre for Computational Informatics, Brisbane, Australia*
[5]*Queensland Institute of Medical Research, Royal Brisbane Hospital Campus, Australia*
[6]*University of Queensland Centre for Clinical Research, Brisbane, Australia*

ABSTRACT: Magnetic resonance imaging (MRI) research in identifying altered brain structure and function in ataxia-telangiectasia, an autosomal recessive neurodegenerative disorder, is limited. Diffusion-weighted MRI were obtained from 11 ataxia telangiectasia patients (age range, 7-22 years; mean, 12 years) and 11 typically developing age-matched participants (age range, 8-23 years; mean, 13 years). Gray matter volume alterations in patients were compared with those of healthy controls using voxel-based morphometry, whereas tract-based spatial statistics was employed to elucidate white matter microstructure differences between groups. White matter microstructure was probed using quantitative fractional anisotropy and mean diffusivity measures. Reduced gray matter volume in both cerebellar hemispheres and in the precentral-postcentral gyrus in the left cerebral hemisphere was observed in ataxia telangiectasia patients compared with controls ($P < 0.05$, corrected for multiple comparisons). A significant reduction in fractional anisotropy in the cerebellar hemispheres, anterior/posterior horns of the medulla, cerebral peduncles, and internal capsule white matter, particularly in the left posterior limb of the internal capsule and corona radiata in the left cerebral hemisphere, was observed in patients compared with controls ($P < 0.05$). Mean diffusivity differences were observed within the left cerebellar hemisphere and the white matter of the superior lobule of the right cerebellar hemisphere ($P < 0.05$). Cerebellum-localized gray matter changes are seen in young ataxia telangiectasia patients along with white matter tract degeneration projecting from the cerebellum into corticomotor regions. The lack of cortical involvement may reflect early-stage white matter motor pathway degeneration within young patients. © 2014 International Parkinson and Movement Disorder Society

Key Words: ataxia telangiectasia; cerebellum; diffusion magnetic resonance imaging; tract-based spatial statistics; voxel-based morphometry

Ataxia telangiectasia (A-T) is an autosomal recessive neurodegenerative disorder that occurs in 1 per 88,000 live births in the United States[1] and in approximately 3 per million live births in the United Kingdom.[2] Multi-system disease characteristics are attributed to genetic mutation of the ATM (ataxia-telangiectasia mutated) gene[3,4] and include progressive cerebellar ataxia, immunodeficiency, sinopulmonary infections, oculocutaneous telangiectasia,[5,6] and elevated serum alpha-fetoprotein levels.[7] The ATM gene encodes the protein kinase ATM, a key player in the cellular response to DNA double-stranded breaks.[8,9] This protein is also involved in the response to oxidative damage, ATM activation by oxidative stress,[10] and it may have a more general role in cell homeostasis. Once activated, ATM phosphorylates a multitude

*Correspondence to: Dr. Stephen E. Rose, CSIRO Centre for Computational Informatics, Level 5, UQ Health Sciences Building, RBWH Herston 4029, Australia, E-mail: Stephen.Rose@csiro.au

Funding agencies: This study was supported by the A-T Children's Project (USA) and BrAshA-T (Australia).

Relevant conflicts of interest/financial disclosures: Nothing to report. Full financial disclosures and author roles may be found in the online version of this article.

Received: 28 January 2014; **Revised:** 15 May 2014; **Accepted:** 16 June 2014

Published online 00 Month 2014 in Wiley Online Library (wileyonlinelibrary.com). DOI: 10.1002/mds.25970

of proteins that control various cellular processes, including different cell cycle checkpoint pathways.[11] Mutation of this gene is linked to increased radiosensitivity in A-T patients[12,13] and in cells from these patients in culture.[14,15] Lymphoreticular malignancy or recurrent chronic respiratory infections[5,6] is the cause of death in most patients.

To date, imaging studies using conventional T1- and T2-weighted magnetic resonance imaging (MRI) have been used to highlight the hallmark neuropathological features associated with A-T, namely progressive cerebellar atrophy.[16-20] Although this has been useful from a radiological perspective, such morphological studies provide limited information of the association between neurodegeneration and the loss in neural motor network integrity. Diffusion-weighted MRI (dMRI), particularly diffusion tensor imaging (DTI), has been demonstrated to allow a more accurate depiction of brain and brainstem structure integrity than that afforded by standard MRI.[21]

In contrast to conventional MRI, DTI measures the random motion of water in cerebral tissue. When this random motion is preferentially restricted to movement in one direction, as occurs along axonal bundles, such diffusion is referred to as anisotropic. Fractional anisotropy (FA) is a quantitative measure of the degree of anisotropy, and mean diffusivity (MD) measures the mean motion of water considered in all directions. White matter (WM) fiber degeneration is typically reflected by decreases in FA, and increases in MD (reviewed in Beaulieu[22]). These measures are used to interrogate pathological changes in regard to myelination, in cerebral tissue.[23] A number of elegant approaches have been developed that enable the voxel-wise analysis of diffusivity measures (FA and MD), such as tract-based spatial statistics (TBSS).[24,25] Furthermore, gray matter (GM) volume can be assessed using voxel-based morphometry (VBM).[26,27] Such analysis strategies have yet to be applied in A-T clinical populations.

Within the research setting, diffusion imaging studies of children with ataxias presents a significant challenge. The most prominent challenge is the presence of excessive image artifacts caused by uncontrolled head motion during nonsedated scanning procedures on diffusion-weighted images. These technical issues have in part been addressed through a series of data preprocessing and correction steps to reduce image distortions inherent to the acquisition technique, as well as those caused by involuntary head movement,[28] allowing dMRI studies to be performed in A-T. Such studies are urgently needed to fully elucidate the relationship between mutation of the ATM gene and loss in the integrity of motor circuitry. The aim of this paper is to highlight the potential of WM and GM imaging, by demonstrating that DTI can be performed successfully on children with A-T. We present novel findings depicting the loss in integrity of key cerebellar-corticomotor pathways with respect to normal brain development in A-T.

Methods

Participants

Magnetic resonance imaging data were acquired from 11 patients with A-T (6 male: age mean $\pm$ SD, 12.18 ± 5.56; age range, 7-22 years) and 11 age-matched typically developing participants (4 male: age mean $\pm$ SD, 12.82 ± 5.51; age range, 8-23 years). All of the patients have been clinically diagnosed for human A-T in accordance with the recent World Health Organization recommendations,[29] including genetic testing. All subjects and parents gave informed consent in accordance with our Human Ethics Institutional Review Board and the Declaration of Helsinki.

Clinical Scoring

The clinical scoring of A-T patients was conducted using a modified version of the A-T Neuro Examination Scale Toolkit (A-T NEST), an A-T scaling system that has been refined from a quantitative 10-point scale since its introduction in 2000.[30] The modified A-T NEST accounts for the multi-dimensional nature of A-T characteristics and compensates for the disease's complexity and heterogeneity, making for an effective and sensitive method to precisely measure A-T neurological deficits (personal communication with Dr. Thomas Crawford, Professor of Neurology and Pediatrics at the John Hopkins Hospital).

Image Acquisition

Imaging data were acquired using a 3T MRI scanner (Siemens Trio, Erlangen, Germany) with TQ gradients (45 mT/m, slew rate 200 T/m/s), using a 12-element Tim head array. A high-resolution structural image was acquired using a 0.9-mm isotropic 3D T1 magnetization prepared rapid gradient echo sequence. The imaging parameters were: field of view, $23 \times 23 \times 17.3$ cm; TR/TE/TI 1,900/2.32/900 ms; flip angle, 9 degrees; matrix size, $192 \times 512 \times 512 \times 1$ cm. Diffusion MRI acquisition consisted of a high angular resolution diffusion imaging (HARDI) sequence with the following parameters: 60 axial slices; 2.5-mm slice thickness; field of view 30×30 cm; TR/TE 9500/116 ms; acquisition matrix 128×128, resulting in an in-plane resolution of 2.34×2.34 mm. Parallel imaging with an acceleration factor of 2 was employed to reduce susceptibility distortions. Sixty-four diffusion-weighted images were acquired at $b = 3{,}000$ s mm^{-2}, along with one minimally diffusion-weighted image ($b = 0$). The acquisition time for the diffusion dataset was 9:40 minutes. A field map for diffusion data was acquired using two

TABLE 1. Summary of clinical observations of A-T patients

Patient	Age	A-T Nest Score	Observed Symptoms
1	16	**Eye movements:** 6/30[a] **Ataxia:** 7/28 **Movement disorder:**2/6 Bradykinesia16/16 Hyperkinesia8/12 Dystonia **Neuropathy:** N/A[b]	**Eye movements:** Off-foveal gaze tendency (vertical or horizontal) is frequent and persistent. Nystagmus on lateral gaze unsustained. **Ataxia:** Sitting requires no support but sways slightly. Standing needs total vertical support. Walking requires vertical support. **Movement disorder:** Hypomimea (dystonic) facial expression and abnormal persistence of large facial expressions. Limb posturing dystonia present with either social/cognitive or motor activation. **Neuropathy:** Absence of ankle tendon, bicep tendon, and knee tendon reflexes. Normal proprioception in toes.
2	7	**Eye movements:** 22/30[a] **Ataxia:** 20/28 **Movement disorder:**3/6 Bradykinesia13/16 HyperkinesiaN/A Dystonia **Neuropathy:** N/A[b]	**Ataxia:** Sitting requires no support but sways slightly. Stands with feet together but sways. Walking has the normal path width without corrective steps. **Neuropathy:** Absence of ankle tendon reflexes. Presence of bicep tendon and knee tendon reflexes. Proprioception in toes and vibration sense at ankles present.
3	12	**Eye movements:** 9/18 **Ataxia:** 8+/26 **Movement disorder:**3.5/8 Bradykinesia6/15 Hyperkinesia10/14 Dystonia **Neuropathy:** N/A[b]	**Eye movements:** Oculo-motor apraxia sometimes observed. **Ataxia:** Sits with self-support of arms. Standing requires no support but takes corrective steps. Walking requires massive lateral support. **Movement disorder:** Retro-colic spasms with motor or stance activation observed. Hypomimea (dystonic) facial expression present. Head/trunk posturing/tilt/turn mild at rest and mild with movement/posture. Trunk posturing/tilt/turn mild at rest and normal with movement/posture.
4	9	**Eye movements:** 19/30 **Ataxia:** 14/28 **Movement disorder:**1/6 Bradykinesia10/16 Hyperkinesia7/11 Dystonia **Neuropathy:** N/A[b]	**Eye movements:** Off-foveal gaze tendency (vertical or horizontal) present only with certain activities. Oculo-motor apraxia present on most (>50%) gaze shifts. Post-rotary nystagmus persists more than 10 seconds. Period alternating nystagmus present. **Ataxia:** Sitting requires no support but sways markedly. Standing takes no support but takes corrective steps. Walking requires no support but wide base or corrective stagger steps taken. **Movement disorder:** Distal/hand tremor present at rest. Proximal (face/head/trunk) tremor present at rest. Hypomimea (dystonic) facial expression present with abnormal persistence of large facial expressions. **Neuropathy:** Normal with proprioception in toes, where movement sensibility is intact.
5	7	**Eye movements:** 29/30 **Ataxia:** 18/28 **Movement disorder:**2/6 Bradykinesia10/16 Hyperkinesia7/11 Dystonia **Neuropathy:** 6/6 (Normal)	**Eye movements:** Off-foveal gaze tendency (vertical or horizontal) present only with certain activities. **Ataxia:** Sitting requires no support but sways slightly/occasionally. Stands with feet together but slight sway. No support required while walking. Walks with normal speed with mild path deviations or corrective steps. **Movement disorder:** Face/head/trunk/distal limb tremor present at rest. Hypomimea (dystonic) facial expression present with abnormal persistence of large expressions.
6	21	Patient had no clinical attendance.	Patient had no clinical attendance.
7	10	**Eye movements:** 17/30 **Ataxia:** 6/28 **Movement disorder:**2/6 Bradykinesia6/16 Hyperkinesia8/11 Dystonia **Neuropathy:** N/A[b]	**Eye movements:** Off-foveal gaze tendency (vertical or horizontal) present only with certain activities. Oculo-motor apraxia present on all gaze shifts. **Ataxia:** Sitting requires no support but sways markedly. Standing requires lateral support. Walking requires massive lateral support. **Movement disorder:** Face/head/trunk/distal limb tremor present with both social/cognitive and motor activation. Hypomimea (dystonic) facial expression present with abnormal persistence of large expressions. Head/trunk posturing present with either social/cognitive or motor activation. **Neuropathy:** Absence of ankle tendon, bicep tendon, and knee tendon reflexes.
8	15	**Eye movements:** 20/30 **Ataxia:** 7/28 **Movement disorder:**1/6 Bradykinesia13/16 Hyperkinesia6/11 Dystonia **Neuropathy:** N/A[b]	**Eye movements:** Horizontal nystagmus unsustained. Nystagmus on lateral gaze unsustained. Off-foveal gaze tendency (vertical or horizontal) present only with certain activities. Oculo-motor apraxia present on most (>50%) gaze shifts. Post-rotary nystagmus persists more than 10 seconds. **Ataxia:** Sitting requires no support but sways markedly. Standing requires vertical support. Walking requires vertical support. **Movement disorder:** Face/head/trunk tremor present with both social/cognitive and motor activation. Hypomimea (dystonic) facial expression present with abnormal persistence of large expressions. Limb posturing present with both social/cognitive and motor activation. Head/trunk posturing present with either social/cognitive or motor activation. **Neuropathy:** Absence of ankle tendon, bicep tendon, and knee tendon reflexes. Proprioception in toes have movement sensibility intact. Some vibration sense present in ankles.

(Continued)

TABLE 1. *Continued*

Patient	Age	A-T Nest Score	Observed Symptoms
9	7	**Eye movements:** 16/30[a] **Ataxia:** 19/28 **Movement disorder:**4/6 Bradykinesia10/14[a] Hyperkinesia8/12 Dystonia **Neuropathy:** 1.5/6	**Ataxia:** Sitting requires no support but sways slightly. Stands with feet together but sways. Walking requires no support. Walks at normal speed with mild deviations in path or corrective steps. **Movement disorder:** Hypomimea (dystonic) facial expression present with abnormal persistence of large expressions. Head posturing and limb posturing present with either social/cognitive or motor activation. **Neuropathy:** Presence of knee tendon reflexes. Absence of ankle tendon reflexes. Proprioception in toes is not completely absent (between scores 0 and 1).
10	22	**Eye movements:** 6/30 **Ataxia:** 5/28 **Movement disorder:**2/6 Bradykinesia8/16 Hyperkinesia3/12 Dystonia **Neuropathy:** N/A[b]	**Eye movements:** Sustained horizontal nystagmus. Sustained nystagmus on lateral gaze. Off-foveal gaze tendency is frequent and persistent. Oculo-motor apraxia is present on all gaze shifts. Post-rotary nystagmus persists more than 10 seconds. **Ataxia:** sitting requires no support but sways slightly. Standing needs support. Walking requires vertical support. **Movement disorder:** Distal limb movement present at rest. Face/head/trunk tremor present with both social/cognitive and motor activation. Hypomimea (dystonic) facial expression present with abnormal persistence of large expressions. Head posturing and limb posturing present with both social/cognitive and motor activation. **Neuropathy:** Absence of ankle tendon, bicep tendon, and knee tendon reflexes. Scored 3 on proprioception and 1 on vibration sense (because proprioception is unreliable), showing that some vibration sense at ankles is intact.
11	8	**Eye movements:** 21/30 **Ataxia:** 7/28[a] **Movement disorder:**2/6 BradykinesiaN/A[b] HyperkinesiaN/A[b] Dystonia **Neuropathy:** 6/6 (normal)	**Eye movements:** Nystagmus on lateral gaze unsustained. Oculo-motor apraxia occasionally present. Post-rotary nystagmus persists more than 10 seconds. Periodic alternating nystagmus present. **Ataxia:** Sitting requires no support but sways markedly. Standing requires no support but takes corrective steps. Walking requires some lateral support.

[a]Not all clinical tests were completed.
[b]Scores are absent/were not recorded.

2-dimensional gradient-recalled echo images (36 axial slices; 3-mm slice thickness with 0.75-mm gap; field of view 19.2 × 19.2 cm; TR/TE1/TE2 488/4.92/7.38 ms; acquisition matrix 64 × 64) to assist correction for distortions caused by susceptibility inhomogeneity.

Diffusion Processing

An extensive preprocessing procedure was followed to detect and correct for image artifacts caused by head motion and image distortions,[28] thereby enabling the use of all patient subjects for analysis. Image volumes affected by within-volume movement were detected using the discontinuity index[31] and excluded from further analysis. Image distortions caused by susceptibility inhomogeneities were reduced using the field map, using tools available with FMRIB's Software Library (FSL[32]). Intensity inhomogeneities were removed using n3.[33] Subsequently, signal intensity outlier voxels (caused by cardiovascular pulsation, bulk head motion, and so forth) were detected and replaced using the detection and replacement of outliers prior to resampling (DROP-R) approach.[34] This involves between-volume registration to account for head movement during the scan time using a fit model to all measurements (FMAM) method,[35] including adjustment of the b-matrix.[36,37] DROP-R was modified from the originally proposed method to employ a model for the detection and replacement of outliers termed higher order model outlier rejection (HOMOR[38]). FA and MD maps were then generated using the MRtrix package.[39]

Tract-Based Spatial Statistics

To investigate WM degeneration between A-T patients and healthy controls, WM microstructure was compared by carrying out voxel-wise statistical analysis of the FA and MD data using TBSS,[24] part of FSL.[25] After alignment of all subjects' FA data into FMRIB58 FA standard-space using the nonlinear registration tool FNIRT,[40,41] the mean FA image was created and thinned to create a mean FA skeleton representing the centers of all tracts common to the group. The aligned FA data of each subject was projected onto this skeleton and the resulting data fed into voxel-wise cross-subject statistics. Permutation-based testing (independent samples *t* test) was carried out using the 'randomize' program included in FSL, which also corrected for multiple comparisons in space, using threshold-free cluster enhancement with 5,000 iterations.[42] Sex was included as a covariate in the analysis. Structures with significantly different FA or MD between subject groups ($P < 0.05$) were identified using the John Hopkins University WM atlases included in FSL.[43]

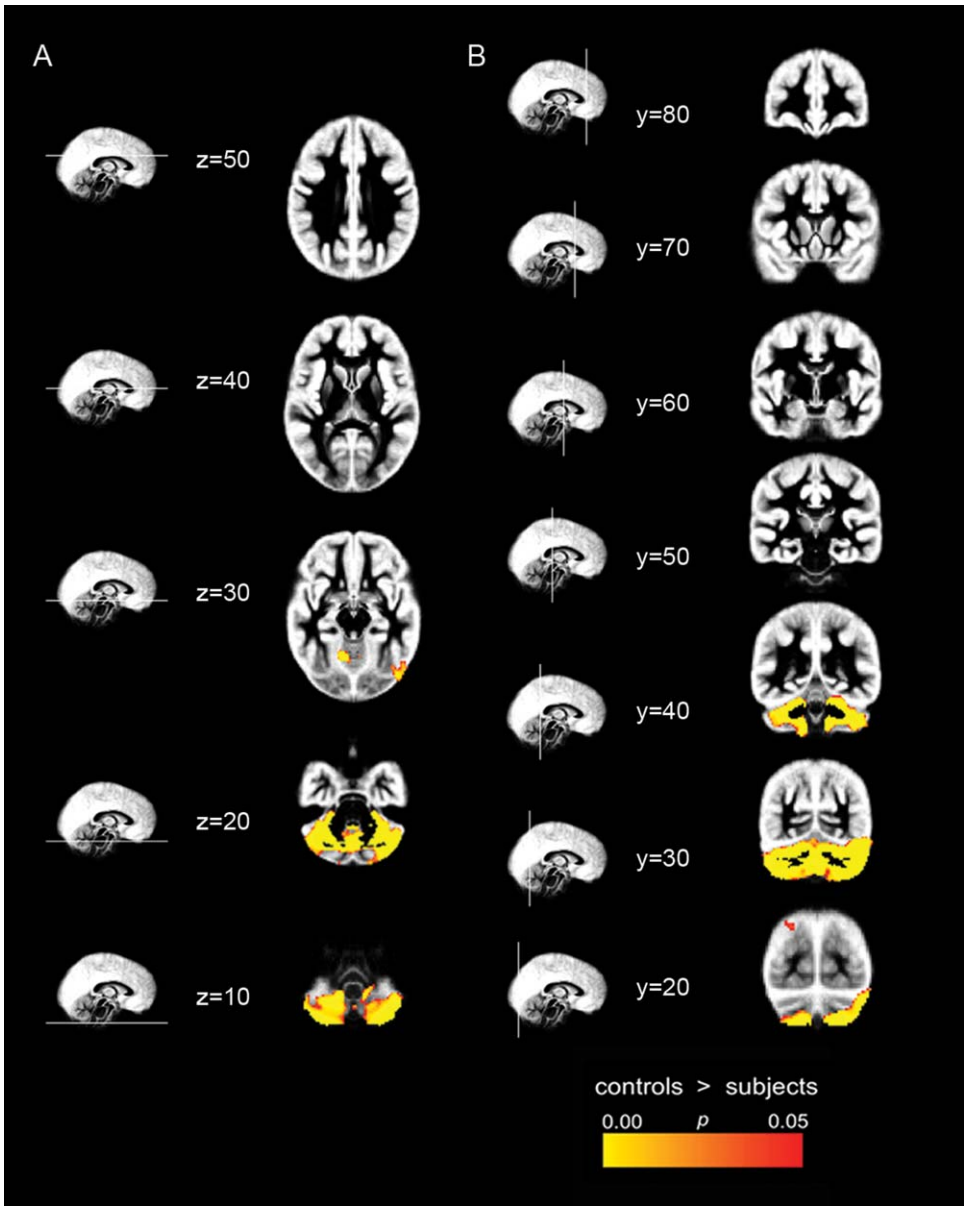

FIG. 1. Axial (**A**) and coronal (**B**) view of voxels with significantly reduced gray matter (GM) volume in ataxia telangiectasia subjects compared with healthy participants. Data are shown at axial and coronal slices of GM template, at Y and Z coordinates as labeled. [Color figure can be viewed in the online issue, which is available at wileyonlinelibrary.com.]

Voxel-Based Morphometry

Gray matter changes between A-T subjects and healthy controls were analyzed with FSL-VBM,[26] an optimized VBM protocol[27] carried out with FSL tools.[25] No A-T subjects were excluded from the analysis based on visual assessment of images for head motion artifacts. Structural images were first brain-extracted and GM-segmented before being nonlinearly registered to the Montreal Neurological Institute (MNI) 152 standard space.[41] A left-right symmetric, study-specific GM template was created using the resulting images, which were averaged and flipped along the x-axis. All native GM images were then nonlinearly registered to this study-specific template and "modulated" for local expansion (or contraction) correction because of the nonlinear component of the spatial transformation. Smoothing with an isotropic Gaussian kernel with a sigma of 3 mm was applied to the modulated GM images. A statistical voxel-wise analysis (independent samples *t* test) was then performed, using permutation-based nonparametric testing with 5,000 iterations, adjusted for multiple comparisons across space, using the threshold-free cluster enhancement.[42] Sex was included as a covariate in the analysis. Voxels were considered significant at corrected $P < 0.05$. We use the terminology *GM volume*, which refers to the likelihood of GM within a voxel, not a physical property of the underlying GM.

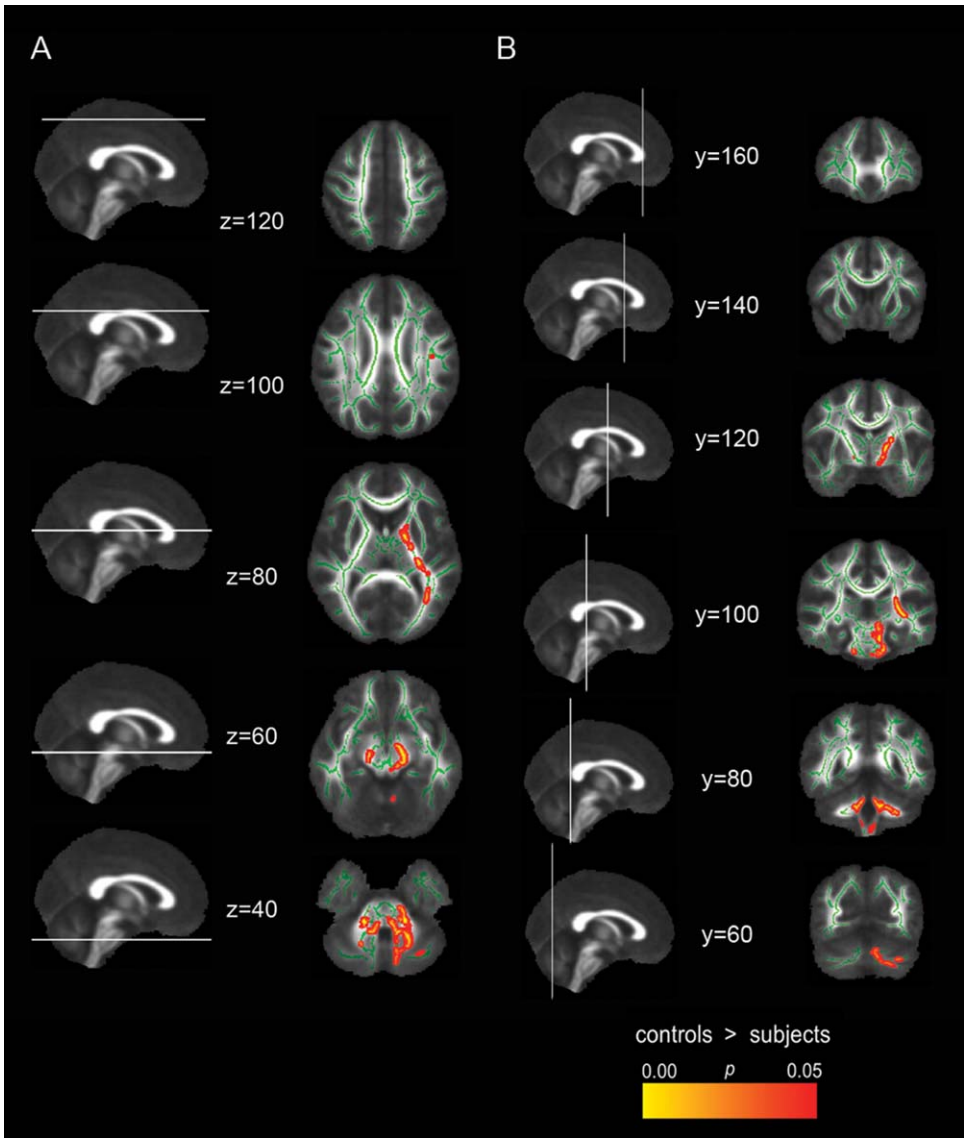

FIG. 2. Axial (**A**) and coronal (**B**) view of voxels with significantly reduced fractional anisotropy (FA) in ataxia telangiectasia subjects compared with healthy participants. Data are shown at labeled MNI-152 Y and Z coordinates overlaid on the mean FA map. Mean FA skeleton is shown in green. [Color figure can be viewed in the online issue, which is available at wileyonlinelibrary.com.]

Results

Clinical and T2-Weighted MRI Observations

T2-weighted MRI axial scans revealed cerebellar atrophy without major pathological conditions in the cerebrum of A-T patients used in this study. WM hyperintensity and telangiectasias (thickening of blood vessels) were not present on T2-weighted MRI (Supplemental Data Fig. 4). Overall, clinical observations indicate heterogeniety of A-T characteristics among patients. Ataxia, movement disorder, and neuropathy were highly individualized in each subject, irrespective of age. Indeed, in the clinical scoring of the A-T cohort, three young patients displayed marked/mixed neuropathy, with a loss of ankle, knee, and bicep tendon reflexes and loss of proprioception in toes (Patients 2, 7, and 9, 7-10 years of age, Table 1), indicating advanced WM degeneration at a young age in the cohort.

Gray Matter Analysis

The VBM analysis revealed areas of reduced GM volume in both the cerebellar hemispheres of the A-T subjects compared with the control participants ($P < 0.05$) (Fig. 1). GM changes were also present in the precentral-postcentral gyrus in the left cerebral hemisphere, indicating possible extension of GM degeneration to the cerebrum. The dentate nucleus was not part of the GM map and was not included in the analysis. The observed changes do not reflect progression of GM degeneration with age and are comparisons made from grouped data from control and A-T data sets.

TABLE 2. Regions that were significantly abnormal in patients with A-T (n = 11) compared with controls (n = 11) after correction for multiple comparisons

DTI Parameters	MNI Coordinates			Cluster Size (voxels)	*P*-Value	Corresponding White Matter Cortical Label (JHU-ICBM-DTI-81 White-Matter Labels Atlas)
	x	y	z			
Reduced FA	x = 129	y = 110	z = 103	7	0.05	Superior longitudinal fasciculus L
	x = 116	y = 106	z = 96	315	0.043	Superior corona radiata L
	x = 111	y = 136	z = 95	3,482	0.023	Superior fronto-occipital fasciculus (could be a part of anterior internal capsule) L
	x = 116	y = 102	z = 95	315	0.043	Posterior corona radiata L
	x = 116	y = 102	z = 90	315	0.043	Posterior limb of internal capsule L
	x = 112	y = 137	z = 90	3,482	0.023	Anterior limb of internal capsule L
	x = 119	y = 112	z = 90	315	0.043	External capsule L
	x =121	y = 67	z = 89	83	0.048	Posterior thalamic radiation (include optic radiation) L
	x = 118	y = 94	z = 87	315	0.043	Retrolenticular part of internal capsule L
	x = 75	y = 117	z = 69	107	0.045	Posterior limb of internal capsule R
	x = 76	y = 117	z = 67	107	0.045	Cerebral peduncle R
	x = 106	y = 112	z = 67	3,482	0.023	Cerebral peduncle L
	x = 95	y = 95	z = 56	3,482	0.023	Superior cerebellar peduncle L
	x = 99	y = 73	z = 51	3,482	0.023	Inferior cerebellar peduncle L
	x = 99	y = 104	z = 50	3,482	0.023	Corticospinal tract L
	x = 79	y = 76	z = 49	14	0.05	Inferior cerebellar peduncle R
	x = 85	y = 82	z = 49	254	0.041	Superior cerebellar peduncle R
	x = 84	y = 93	z = 47	254	0.041	Medial lemniscus R
	x = 104	y = 102	z = 47	3,482	0.023	Middle cerebellar peduncle
	x = 97	y = 92	z = 47	3,482	0.023	Medial lemniscus L
	x = 95	y = 94	z = 37	3,482	0.023	Pontine crossing tract (a part of MCP)
Increased MD	x = 109	y = 74	z = 43	1,402	0.009	Middle cerebellar peduncle
	x = 79	y = 78	z = 51	224	0.032	Inferior cerebellar peduncle R
	x = 96	y = 75	z = 50	1,402	0.009	Inferior cerebellar peduncle L

White Matter Analysis

The TBSS analysis showed a significant reduction in FA in a number of WM tracts in the A-T subjects compared with the control participants. As shown in Figure 2, these regions included the cerebellar hemispheres, anterior/posterior horns of the medulla, cerebral peduncles, and WM of the internal capsule, particularly involving the left posterior limb of the internal capsule and corona radiata in the left cerebral hemisphere ($P < 0.05$); see Table 2 for a summary of imaging findings. Differences in MD were observed within the left cerebellar hemisphere and the WM of the superior lobule of the right cerebellar hemisphere ($P < 0.05$) (Fig. 3). Significant loss in integrity of cerebellar WM and degeneration of WM tracts projecting from the cerebellum into corticomotor regions is collectively seen. The observed changes do not reflect progression of WM degeneration with age and are comparisons made from grouped data from control and A-T data sets.

Discussion

Diffusion-weighted MRI, the method of choice for investigating cerebellar WM degeneration associated with multi-spectrum ataxic disorders,[44-46] has not yet been extended to the study of A-T. An important outcome of the current study is to highlight that, with use of an appropriate analysis pipeline, it is possible to study the WM microstructure of key cerebellar-corticomotor pathways within a sizeable A-T patient age range. Furthermore, voxel-wise TBSS and VBM analyses enabled delineation of WM and GM changes in the cerebrum and cerebellum of A-T subjects compared with control participants that are similar to neuropathological features reported in postmortem studies.[47-53]

The novel finding from this study identifies the degeneration of important cerebellar-corticomotor pathways responsible for coordinated motor function in all A-T patients analyzed. The results of the VBM analysis demonstrate that GM changes are localized primarily to the cerebellum in these patients. Note that our analysis consisted of young children with A-T, in whom, generally, GM changes are rarely seen.[48,51-53] Serial qualitative analysis of high-resolution MRI data was not performed in this study and so trajectories of GM changes with age is yet to be established in A-T. In addition, correlation of VBM results with clinical scores was not performed, because scoring was incomplete (Table 1). Additional studies using VBM should focus on the inclusion of older A-T patients (late second decade and older), with appropriate age- and sex-matched control participant data, to provide a more comprehensive insight of GM

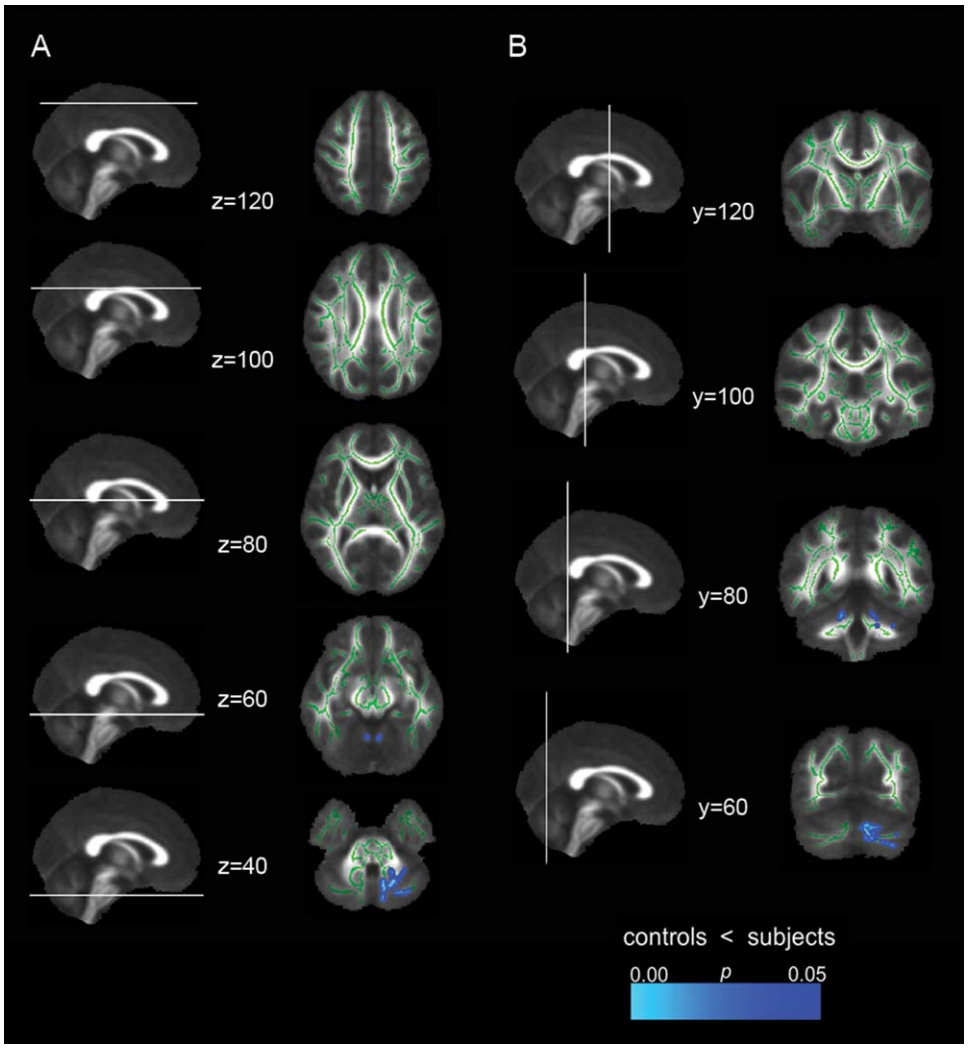

FIG. 3. Axial (**A**) and coronal (**B**) view of voxels with significantly different mean diffusivity (MD) between healthy and ataxia telangiectasia subjects. Data are shown at labeled MNI-152 Y and Z coordinates overlaid on the mean FA map. Mean FA skeleton is shown in green. [Color figure can be viewed in the online issue, which is available at wileyonlinelibrary.com.]

changes with age. We predict more pronounced GM changes would be observed in an older A-T cohort, as suggested from reported postmortem findings.[51]

In terms of WM, we show changes associated with a number of cerebellar-corticomotor pathways, predominately within the left hemisphere in our A-T subjects. The localization of changes to the dominant hemisphere is not clear. Postmortem studies, in general, have not focused on neurodegenerative laterality. In one study, hemorrhagic lesions in left occipital WM were recorded in a 26-year-old male A-T patient.[49] In a recent similar study of Friedreich's ataxia using TBSS and VBM, increased MD was observed in the WM underlying the left central sulcus, among other general findings. A decrease in FA in the left superior cerebellar peduncle correlated with clinical severity.[54] Whether the localized WM changes in the left hemisphere are cohort specific or reflect more early degenerative changes in young A-T patients is unclear. Despite clinical observations of extensive WM neurodegeneration in young A-T sufferers in our study cohort, no clear correlation has been seen between this clinical observation and our imaging findings.

We also show a significant reduction in FA in the cerebral peduncles and WM of the internal capsule, particularly involving the left posterior limb of the internal capsule and corona radiata in the left cerebral hemisphere in A-T patients. These findings were not reflected in structural T2-weighted axial scans (Supplemental Data Fig. 4), indicating the sensitivity and specificity of dMRI for delineating WM degeneration. Our radiological findings in general do not reflect past imaging observations in cerebral pathological conditions in A-T.[19] As seen from clinical observations of our A-T cohort, A-T neuropathology can be heterogeneous in nature among different patients, irrespective of age[20,55,56]; therefore, disease characteristics may differ from cohort to cohort.

Multisite studies with larger cohorts of A-T subjects may provide improved insight into the degeneration of WM pathways and the neurological variability associated with the disease. To broaden our perspective of the impact of mutation in the ATM gene, the temporal trajectories of WM and GM changes with age should be further investigated, particularly in older patients, because this important information is yet to be established in A-T. In addition to this, serial evaluation of WM and GM changes with age in individual A-T subjects should be investigated in the future to understand whether these changes are caused by degeneration or delayed WM and GM maturation. Together, with VBM results, our TBSS findings support a mechanism of degeneration within the cerebellum, propagating to corticomotor regions along the length of the cortico-cerebellar motor pathways.

Future studies also should investigate degeneration of motor pathways that involve subcortical structures such as the basal ganglia, which are known to be involved with motor disorders. Basal ganglia pathological conditions were not explicitly seen in our study, despite the array of A-T characteristics observed in our clinical observations (Table 1); however, abnormalities in this structure have been previously recorded both in postmortem study[50] and in radiological findings,[57] particularly in older patients. As we have already mentioned, our particular A-T cohort consisted of very young patients; therefore, future work in A-T should include older A-T subjects as well as younger patients to provide an age-specific timeline of neuropathology in A-T.

This study has a number of limitations, the foremost being the small number of A-T participants to undergo analysis and the impact on our findings. Australia has seen fewer than 50 cases of A-T overall,[58] with our clinic being the only research clinic nationally, specializing in health care for 11 of those A-T patients, representing 22% of the national population. The groupwise analysis strategies employed in this study also make it difficult to fully understand the heterogeneity of patterns of degeneration across A-T subjects. In our clinic, we observed heterogeneity of movement disorders in each patient (Table 1), which suggests that A-T affects not only cerebellar tracts but many other motor circuits. The extent of multiple affected areas of the brain and their sequence of development will only be realized with much larger collaborative studies across multiple research sites.[59]

Future dMRI studies also could employ probabilistic tractography to delineate WM fiber tracts, to allow the connectivity and integrity of specific WM pathways linking multiple brain regions to be assessed.[60,61] Such technology has been used in a number of ataxic conditions to study cerebellar-corticomotor networks[44-46] and are urgently required to fully understand the impact of ATM gene mutation and loss in connectivity of A-T motor circuits. ■

Acknowledgments: We thank the A-T Children's Project (USA) and BrAshA-T (Australia) for their funding support, Prof Roslyn Boyd of the Queensland Cerebral Palsy and Rehabilitation Research Centre for the provision of control participants in our study, Ms Kate Munro of the Neurosciences Department in the Queensland Royal Children's Hospital for providing clinical support, Dr. Thomas Crawford, Professor of Neurology and Pediatrics at the John Hopkins Hospital (USA), and Ms Cynthia Rothblum-Oviatt of the A-T Children's Project (USA) for their insight and clarification of the A-T NEST clinical scoring system, and Aiman Al Najjar and Anita Burns of the University of Queensland Centre of Advanced Imaging (CAI) for their assistance in acquisition of the MRI data.

References

1. Swift M, Morrell D, Cromartie E, Chamberlin AR, Skolnick MH, Bishop DT. The incidence and gene frequency of ataxia-telangiectasia in the United States. Am J Hum Genet 1986;39:573-583.
2. Woods CG, Bundey SE, Taylor AM. Unusual features in the inheritance of ataxia telangiectasia. Hum Genet 1990;84:555-562.
3. Gatti RA, Berkel I, Boder E, et al. Localization of an ataxia-telangiectasia gene to chromosome 11q22-23. Nature 1988;336:577-580.
4. Savitsky K, Bar-Shira A, Gilad S, et al. A single ataxia telangiectasia gene with a product similar to PI-3 kinase. Science 1995;268:1749-1753.
5. Boder E, Sedgwick RP. Ataxia-telangiectasia: a familial syndrome of progressive cerebellar ataxia, oculocutaneous telangiectasia and frequent pulmonary infection. Pediatrics 1958;21:526-554.
6. Dunn HG, Meuwissen H, Livingstone CS, Pump KK. ATAXIA-TELANGIECTASIA. Can Med Assoc J 1964;91:1106-1118.
7. Waldmann TA, McIntire KR. Serum-alpha-fetoprotein levels in patients with ataxia-telangiectasia. Lancet 1972;2:1112-1115.
8. Lavin MF. Ataxia-telangiectasia: from a rare disorder to a paradigm for cell signalling and cancer. Nat Rev Mol Cell Biol 2008;9:759-769.
9. Shiloh Y, Ziv Y. The ATM protein kinase: regulating the cellular response to genotoxic stress, and more. Nat Rev Mol Cell Biol 2013;14:197-210.
10. Guo Z, Kozlov S, Lavin MF, Person MD, Paull TT. ATM activation by oxidative stress. Science 2010;330:517-521.
11. Beamish H, Williams R, Chen P, Lavin MF. Defect in multiple cell cycle checkpoints in ataxia-telangiectasia postirradiation. J Biol Chem 1996;271:20486-20493.
12. Gotoff SP, Amirmokri E, Liebner EJ. Ataxia telangiectasia: neoplasia, untoward response to x-irradiation, and tuberous sclerosis. Am J Dis Child 1967;114:617-625.
13. Morgan JL, Holcomb TM, Morrissey RW. Radiation reaction in ataxia telangiectasia. Am J Dis Child 1968;116:557-558.
14. Taylor AM, Harnden DG, Arlett CF, et al. Ataxia telangiectasia: a human mutation with abnormal radiation sensitivity. Nature 1975;258:427-429.
15. Chen PC, Lavin MF, Kidson C, Moss D. Identification of ataxia telangiectasia heterozygotes, a cancer prone population. Nature 1978;274:484-486.
16. Farina L, Uggetti C, Ottolini A, et al. Ataxia-telangiectasia: MR and CT findings. J Comput Assist Tomogr 1994;18:724-727.
17. Kamiya M, Yamanouchi H, Yoshida T, et al. Ataxia telangiectasia with vascular abnormalities in the brain parenchyma: report of an autopsy case and literature review. Pathol Int 2001;51:271-276.
18. Tavani F, Zimmerman RA, Berry GT, Sullivan K, Gatti R, Bingham P. Ataxia-telangiectasia: the pattern of cerebellar atrophy on MRI. Neuroradiology 2003;45:315-319.
19. Lin DD, Barker PB, Lederman HM, Crawford TO. Cerebral abnormalities in adults with ataxia-telangiectasia. AJNR Am J Neuroradiol 2013;35:119-123.
20. Huang Y, Yang L, Wang JC, et al. Twelve novel Atm mutations identified in Chinese ataxia telangiectasia patients. Neuromol Med 2013;15:536-540.

21. Sood S, Gupta A, Tsiouris AJ. Advanced magnetic resonance techniques in neuroimaging: diffusion, spectroscopy, and perfusion. Semin Roentgenol 2010;45:137-146.
22. Beaulieu C. The basis of anisotropic water diffusion in the nervous system: a technical review. NMR Biomed 2002;15:435-455.
23. Alexander AL, Lee JE, Lazar M, Field AS. Diffusion tensor imaging of the brain. Neurotherapeutics 2007;4:316-329.
24. Smith SM, Jenkinson M, Johansen-Berg H, et al. Tract-based spatial statistics: voxelwise analysis of multi-subject diffusion data. Neuroimage 2006;31:1487-1505.
25. Smith SM, Jenkinson M, Woolrich MW, et al. Advances in functional and structural MR image analysis and implementation as FSL. Neuroimage 2004;23(Suppl 1):S208-S219.
26. Douaud G, Smith S, Jenkinson M, et al. Anatomically related grey and white matter abnormalities in adolescent-onset schizophrenia. Brain 2007;130(Pt 9):2375-2386.
27. Good CD, Johnsrude IS, Ashburner J, Henson RN, Friston KJ, Frackowiak RS. A voxel-based morphometric study of ageing in 465 normal adult human brains. Neuroimage 2001;14:21-36.
28. Pannek K, Guzzetta A, Colditz PB, Rose SE. Diffusion MRI of the neonate brain: acquisition, processing and analysis techniques. Pediatr Radiol 2012;42:1169-1182.
29. Notarangelo L, Casanova JL, Fischer A, et al. Primary immunodeficiency diseases: an update. J Allergy Clin Immunol 2004;114: 677-687.
30. Crawford TO, Mandir AS, Lefton-Greif MA, et al. Quantitative neurologic assessment of ataxia-telangiectasia. Neurology 2000;54: 1505-1509.
31. Nam H, Park HJ. Distortion correction of high b-valued and high angular resolution diffusion images using iterative simulated images. Neuroimage 2011;57:968-978.
32. Jenkinson M, Beckmann CF, Behrens TE, Woolrich MW, Smith SM. FSL. Neuroimage 2012;62:782-790.
33. Sled JG, Zijdenbos AP, Evans AC. A nonparametric method for automatic correction of intensity nonuniformity in MRI data. IEEE Trans Med Imaging 1998;17:87-97.
34. Morris D, Nossin-Manor R, Taylor MJ, Sled JG. Preterm neonatal diffusion processing using detection and replacement of outliers prior to resampling. Magn Reson Med 2011;66:92-101.
35. Bai Y, Alexander P. Model-based registration to correct for motion between acquisitions in diffusion MR imaging. IEEE International Symposium on Biomedical Imaging: From Nano to Macro; 2008.
36. Rohde GK, Barnett AS, Basser PJ, Marenco S, Pierpaoli C. Comprehensive approach for correction of motion and distortion in diffusion-weighted MRI. Magn Reson Med 2004;51:103-114.
37. Leemans A, Jones DK. The B-matrix must be rotated when correcting for subject motion in DTI data. Magn Reson Med 2009; 61:1336-1349.
38. Pannek K, Raffelt D, Bell C, Mathias JL, Rose SE. HOMOR: higher order model outlier rejection for high b-value MR diffusion data. Neuroimage 2012;63:835-842.
39. Tournier JD, Calamante F, Connelly A. MRtrix: Diffusion tractography in crossing fiber regions. International Journal of Imaging Systems and Technology 2012;22:53-66.
40. Andersson JLR, Jenkinson M, Smith S. Non-linear optimization FMRIB Technial Report TR07JA1. Oxford, United Kingdom: FMRIB Centre; 2007.
41. Andersson JLR, Jenkinson M, Smith S. Non-linear registration, aka Spatial normalisation. FMRIB technical report TR07JA2 from www.fmrib.ox.ac.uk/analysis/techrep: FMRIB; 2007.
42. Smith SM, Nichols TE. Threshold-free cluster enhancement: addressing problems of smoothing, threshold dependence and localisation in cluster inference. Neuroimage 2009;44:83-98.
43. Hua K, Zhang J, Wakana S, et al. Tract probability maps in stereotaxic spaces: analyses of white matter anatomy and tract-specific quantification. Neuroimage 2008;39:336-347.
44. Habas C, Cabanis EA. Anatomical parcellation of the brainstem and cerebellar white matter: a preliminary probabilistic tractography study at 3 T. Neuroradiology 2007;49:849-863.
45. Pagani E, Ginestroni A, Della Nave R, et al. Assessment of brain white matter fiber bundle atrophy in patients with Friedreich ataxia. Radiology 2010;255:882-889.
46. Prodi E, Grisoli M, Panzeri M, et al. Supratentorial and pontine MRI abnormalities characterize recessive spastic ataxia of Charlevoix-Saguenay: a comprehensive study of an Italian series. Eur J Neurol 2013;20:138-146.
47. Verhagen MM, Martin JJ, van Deuren M, et al. Neuropathology in classical and variant ataxia-telangiectasia. Neuropathology 2012;32:234-244.
48. De Leon GA, Grover WD, Huff DS. Neuropathologic changes in ataxia-telangiectasia. Neurology 1976;26:947-951.
49. Monaco S, Nardelli E, Moretto G, Cavallaro T, Rizzuto N. Cytoskeletal pathology in ataxia-telangiectasia. Clin Neuropathol 1988; 7:44-46.
50. Terplan KL, Krauss RF. Histopathologic brain changes in association with ataxia-telangiectasia. Neurology 1969;19:446-454.
51. Sourander P, Bonnevier JO, Olsson Y. A case of ataxia-telangiectasia with lesions in the spinal cord. Acta Neurol Scand 1966;42:354-366.
52. Solitare GB. Louis-Bar's syndrome (ataxia-telangiectasia): anatomic considerations with emphasis on neuropathologic observations. Neurology 1968;18:1180-1186.
53. Aguilar MJ, Kamoshita S, Landing BH, Boder E, Sedgwick RP. Pathological observations in ataxia-telangiectasia: a report of five cases. J Neuropathol Exp Neurol 1968;27:659-676.
54. Della Nave R, Ginestroni A, Tessa C, et al. Brain white matter tracts degeneration in Friedreich ataxia. An in vivo MRI study using tract-based spatial statistics and voxel-based morphometry. Neuroimage 2008;40:19-25.
55. Perlman S, Becker-Catania S, Gatti RA. Ataxia-telangiectasia: diagnosis and treatment. Semin Pediatr Neurol 2003;10:173-182.
56. Chun HH, Gatti RA. Ataxia-telangiectasia, an evolving phenotype. DNA Repair 2004;3:1187-1196.
57. Kieslich M, Hoche F, Reichenbach J, et al. Extracerebellar MRI-lesions in ataxia telangiectasia go along with deficiency of the GH/IGF-1 axis, markedly reduced body weight, high ataxia scores and advanced age. Cerebellum 2010;9:190-197.
58. Miles J. A charity that begins at home. The Courier-Mail 2011 November 12, 2011.
59. Anscombe C. New technology could shed light on treatment of rare genetic condition In. 375/13 ed. The University of Nottingham, University Park, Nottingham; 2013.
60. Ciccarelli O, Behrens TE, Altmann DR, et al. Probabilistic diffusion tractography: a potential tool to assess the rate of disease progression in amyotrophic lateral sclerosis. Brain 2006;129:1859-1871.
61. Johansen-Berg H, Rushworth MF. Using diffusion imaging to study human connectional anatomy. Annu Rev Neurosci 2009;32: 75-94.

Supporting Data

Additional supporting information may be found in the online version of this article at the publisher's web-site.